Spectrum and Structure of Excited Nucleons from Exclusive Electroproduction

V. Burkert,[1] R. Gothe,[2] V. Mokeev,[1] C. D. Roberts,[3] and A. Szczepaniak[4]

[1] *Thomas Jefferson National Accelerator Facility, Newport News, VA 23606, USA*
[2] *Department of Physics and Astronomy, University of South Carolina, Columbia, SC 29208, USA*
[3] *Physics Division, Argonne National Laboratory, Argonne, IL 60439, USA*
[4] *Department of Physics, Indiana University, Bloomington, IN 47405, USA*

(Dated: September 29, 2017)

Two of the most basic goals of nuclear physics are to understand the mechanisms responsible for the formation of hadrons and explain their structure in terms of the gluons and quarks of quantum chromodynamics (QCD). In this connection, measurements of the nucleon excitation (N^*) spectrum and exploration of N^* structure through the study of resonance electroexcitation amplitudes ($\gamma_v N N^*$ electrocouplings) on a broad domain of photon virtualities (Q^2) present unique opportunities for elucidating these crucial aspects of nonperturbative strong-interaction dynamics. The complexity of this problem is great, so a multipronged approach is necessary to achieve its solution. A workshop entitled "Spectrum and Structure of Excited Nucleons from Exclusive Electroproduction" was therefore planned, and it took place in the week 14-18 November 2016 at the Institute for Nuclear Theory (INT Workshop INT-16-62W). A key aim of this workshop was to facilitate interactions between expert practitioners representing the various, complementary approaches to this problem. The workshop gathered more than 30 participants, and explored themes ranging from basic theory through practical phenomenology and onto the means by which conjectures and predictions can be verified empirically via studies of exclusive electroproduction. This document is a summary of the contributions. It was acknowledged that the range and impact of this program will be greatly expanded by experiments enabled by the CLAS12 detector in the new JLab12 era.

CONTENTS

I. Experiment 1
A. Search for new excited baryons 1
B. Structure of baryon resonances 1
C. Resonance production at 12 GeV 3
D. Future searches for hybrid baryon states 3

II. Constituent Quark Models 3
A. Successes 3
B. Challenges 5

III. Dyson-Schwinger Equations 5

IV. Lattice QCD 8

V. Reaction Theory 10

VI. Future 11

References 12

I. EXPERIMENT

A. Search for new excited baryons

During the past decade tremendous amounts of new meson photo- and electroproduction data have been accumulated and some of them have already been subjected to detailed analyses in the quest for undiscovered excited baryon states in the sector of light quarks [1–4]. The data sets contain high statistics differential cross section results as well as many polarization observables obtained from polarized beams, polarized nucleon targets, and recoil polarization measurements. While many data sets are still waiting to be included in multi-channel partial wave analyses, e.g. vector meson channels, a set of new baryon states has been discovered based on the information carried by the new data and has been included in the recent Review of Particle Properties (RPP) edition [5]. Reviews of the ongoing experimental efforts at CBELSA/TAPS and CLAS have been presented at the INT-16-62W workshop in Seattle. The production of $N\pi$ final states is known to be less sensitive to resonance excitations at high masses. At this workshop, however, the example of the $\Delta(2200)\frac{7}{2}^-$ resonance has been used to show that the (relative) simplicity of the process combined with very high statistics data and the availability of multiple polarization observables provides powerful constraints that allow for the confirmation of known states (as in the case of the poorly known $\Delta(2200)\frac{7}{2}^-$) and possibly the discovery of new states, even if the $N\pi$ coupling is only of the order of a few percent. At CBELSA/TAPS, in addition to single neutral meson final states, like $\gamma p \to p\pi^\circ$ and $p\eta$, recently also multi-particle final states, like $p\pi^\circ\pi^\circ$ and $p\pi^\circ\eta$ and $\gamma D \to n\eta(p)$ reactions, have been measured, including polarization asymmetries [6–10]. These new data are now included in coupled channel partial wave analyses and searches for new excited N^* and Δ^* states.

B. Structure of baryon resonances

Most experimental presentations focused on the status and future prospects of data in the single pion, eta,

kaon, and two-pion electroproduction [11, 12]. This included new preliminary data of pion electroproduction off neutrons [13]. Meson electroproduction has been of particular interest at this INT workshop, as the Q^2 dependence of the $\gamma_v NN^*$ transition helicity amplitudes, or electrocouplings, provides fundamental information on their continuous evolution with distance scale and hence on the varying effective degrees of freedom, which are uniquely intertwined with the structure of each individual resonance, accessing many facets of the strong QCD dynamics that is responsible for the generation of all hadronic states. These fundamental quantities are now subject to computations starting from theoretical approaches based on the QCD Lagrangian. Studies of the CLAS results on the $\Delta(1232)\frac{3}{2}^+$ and $N(1440)\frac{1}{2}^+$ electrocouplings [14–16] within the Dyson Schwinger Equation (DSE) approach [17] have demonstrated the capability to access the momentum-dependent evolution of the dressed quark mass. This fundamental ingredient of strong QCD elucidates the emergence of the overwhelming part (>98%) of the hadron mass. These studies of the N^* structure are therefore of particular importance for contemporary hadron physics.

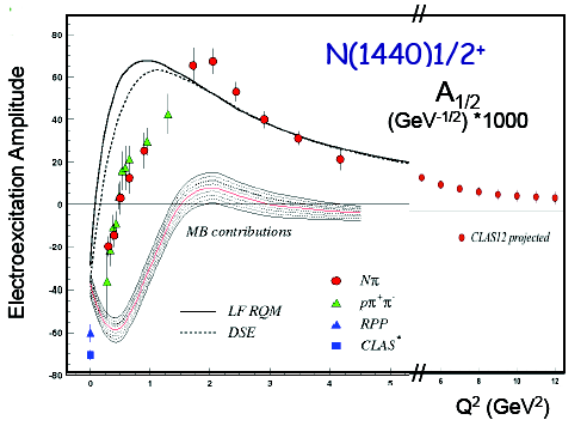

FIG. 1. Description of the CLAS results on N(1440)$1/2^+$ $A_{1/2}$ electrocouplings [14–16] within the framework of DSE [17] and a light-front quark model [25] that both employ a momentum-dependent mass for the dressed constituent quarks. Meson-baryon cloud contributions are estimated by the difference between experimental data and the DSE predictions for the quark core contributions. Projected results for the experiments with CLAS12 [22] are also shown as red bullets.

Exclusive single pion electroproduction off protons is used as a powerful tool to probe the effective degrees of freedom in several excited nucleon states at varying distance scales. The analysis of the $ep \to en\pi^+$ reaction has been carried out using dedicated experimental data, taken at 6-GeV beam energy. Helicity transition amplitudes for several resonances have been mapped out. These include the $N(1440)\frac{1}{2}^+$, $N(1520)\frac{3}{2}^-$, $N(1535)\frac{1}{2}^-$, $N(1675)\frac{5}{2}^-$, $N(1680)\frac{5}{2}^+$, and $N(1710)\frac{1}{2}^+$ nucleon excited states [14, 18]. These states could be isolated in single-channel analyses as there are no close by Δ^* states to contaminate the isospin $\frac{1}{2}$ partial waves with isospin $\frac{3}{2}$ contributions in the same partial wave. Some of these results are now included in the recent RPP edition [5]. However, in order to determine amplitudes of other resonant partial waves, additional information from the $p\pi^\circ$ final state is needed. This final state couples preferentially to Δ^* states, and data in this final state are needed for a combined two-channel analysis to separate N^* and Δ^* resonances with same J^P quantum numbers that are in the same mass region. This will allow an isospin separation of states in the so-called 3^{rd} resonance region with masses near 1700 MeV, as for example for the J^P doublets $N(1650)\frac{1}{2}^-$, $\Delta(1620)\frac{1}{2}^-$ and $N(1700)\frac{3}{2}^-$, $\Delta(1700)\frac{3}{2}^-$, for which insufficient information is available to separate them from each other. A full isospin decomposition of the resonance amplitudes can only be achieved by measuring one more distinct final state, such as $p\pi^-$, which will also allow for the first time to verify theoretical predictions of quark-flavor separated electroexcitation amplitudes.

High statistics data have been measured in the $ep \to e'p'\pi^\circ$ and $en(p) \to e'p'\pi^-(p)$ exclusive channels with CLAS in the photon virtuality range $Q^2 = 0.4 - 1.0$ GeV^2 and the invariant mass range of the $N\pi$ system $W = 1.1{-}1.8$ GeV [13]. The structure functions $\sigma_T + \epsilon\sigma_L$, σ_{TT}, and σ_{LT} have been extracted and preliminary results were presented. For the fully exclusive $p\pi^-$ final state, the quasi-free electroproduction cross sections off the bound neutron and the final-state-interaction contributions have been kinematically isolated and determined in each accessible four-dimensional phase space bin. First $\pi^+\pi^- p$ electroproduction cross sections off protons bound in deuterium [19] are now also becoming available from the same measurement and will expand, in comparison with the free proton results, our knowledge on how nuclear effects impact the extracted $\gamma_v NN^*$ transition helicity amplitudes. Moreover, the high degree of the electron beam polarization in this measurement allowed the extraction of the electron spin asymmetry and polarized structure function $\sigma_{LT'}$ in the $p\pi^\circ$ channel. These preliminary data, in combination with the results of the $\pi^+ n$ channel, will significantly extend our knowledge on N^* electroproduction throughout the resonance region. Further preliminary cross section and structure function results were presented for the exclusive $ep \to ep\pi^\circ$ reaction in the resonance region up to W = 2 GeV at higher photon virtualities Q^2 between 2.4 and 6 GeV^2. They will complement the already available $n\pi^+$ data in the same W and Q^2 range and will provide high statistics data in this intermediate mass and Q^2 range.

Resonance extractions from cross section and polarization data are a complex process and involve some model uncertainties. It is thus highly desirable that resonance transitions are determined from more than just one final state, e.g. $N\pi$. This will demonstrate the consis-

tency of the results, as the resonance parts should be the same but the non-resonant contributions are very different. For some selected resonances, e.g. $N(1440)\frac{1}{2}^+$ and $N(1520)\frac{3}{2}^+$ shown in Figs. 1 and 2, which have significant couplings to two different final states, i.e. $N\pi$ and $\pi^+\pi^- p$, electrocouplings have been extracted from both channels independently, showing excellent consistency [14–16]. These results support, that a reliable extraction of these fundamental quantities from electroproduction data is possible. The same consistency has also been seen for the $N(1535)\frac{1}{2}^-$ resonance (Fig. 2), which has been analyzed using both $n\pi^+$ and $p\eta$ data samples, independently [14, 20]. In the case of the $n\pi^+$ final state two different analysis approaches, a unitary isobar and a dispersion relation one, have been applied to the same data set leading also to consistent results. Furthermore, the $\Delta(1620)\frac{1}{2}^-$, $\Delta(1700)\frac{3}{2}^-$, and $N(1720)\frac{3}{2}^+$ resonances, as many other higher-lying resonances, decay dominantly into $N\pi\pi$ final states, making the exclusive $\pi^+\pi^- p$ electroproduction off protons a major source of information on the electrocouplings of these states. First results on the electrocouplings as well as the $\pi\Delta$ and ρp hadronic decay widths of the $\Delta(1620)\frac{1}{2}^-$ resonance have been recently extracted from CLAS data and were presented at this meeting [16].

In the near future, electrocouplings of N^*s with masses up to 2.0 GeV will also become available at $Q^2 < 5.0$ GeV^2 from the πN and $\pi^+\pi^- p$ electroproduction data off protons [16, 21]. This will allow for the extraction of orbital excited states in the [70,1$^-$] and [56,2$^+$] multiplets, as for example the $\Delta(1950)\frac{7}{2}^+$ resonance, which is expected to couple strongly to both $N\pi$ and $N\pi\pi$ final states.

C. Resonance production at 12 GeV

While the currently available data from the experimental 6-GeV electroproduction program at CLAS provides only a glimpse of the running quark mass, future results on resonance electrocouplings from CLAS12 will expand the kinematic range up to $Q^2 \leq 12$ GeV^2 [22–24]. It will then be possible to extend the exploration of the dressed quark mass function to distance scales, where the transition from strong QCD to perturbative QCD occurs, allowing us to address the most challenging open problems in hadron physics on the nature of the hadron mass, quark-gluon confinement, and their emergence from QCD.

D. Future searches for hybrid baryon states

Gluonic excitations of baryons (hybrid baryons) have been explored theoretically and predictions of hybrid baryon masses and quantum numbers have recently been made in Lattice QCD (LQCD) [28]. In distinction to the meson sector, hybrid baryons have the same quantum numbers as regular three-quark baryons, therefore they cannot be identified just by their quantum numbers. However, the hybrid baryon configuration q^3G incorporates additional glue in the wave function and is in quark models expected to have transition form factors that behave very differently than those of a q^3 quark state that otherwise has the same quantum numbers. For example, for the lowest-mass Roper-like hybrid baryon with spin-parity $J^P = \frac{1}{2}^+$, the scalar amplitude is predicted to be zero and the transverse amplitude $A_{1/2}$ should drop rapidly with Q^2, while both is not expected for the equivalent q^3 state [29]. This is due to the different internal structure of the two states. These circumstances are exploited in the planned experimental program with CLAS12, that uses even higher luminosities than previously available to measure several reactions, such as $K^+\Lambda$, $N\pi$, $p\pi^+\pi^-$, and others, to search for new states in the mass range from 2.0 to 3.0 GeV and to extract their transition helicity amplitudes at lower Q^2, where hybrid baryon contributions are expected to be most prominent [30].

Presentations: Volker Burkert, Philip Cole, Annalisa D'Angelo, Ralf Gothe, Kenneth Hicks, Nikolay Markov, Viktor Mokeev, Kijun Park, Ulrike Thoma, and Maurizio Ungaro.

II. CONSTITUENT QUARK MODELS

A. Successes

Constituent quark models are currently an important tool that provides a first step in relating $\gamma_{r,v}pN^*$ photo-/electrocouplings from the experimentally available data over a wide spectrum of the nucleon resonances to strong QCD dynamics. The measured baryon quantum numbers and spectrum appear consistent with those predicted by quark models that employ $SU(6)\otimes O(3)$ symmetry. This pattern is further supported by the lattice-QCD (lQCD) evaluation of the N* spectrum [31]. Some of the "missing" N^* resonances predicted by the quark model have recently been uncovered through partial wave analyses of high statistics data, as presented at this meeting, and resonances with different spin appear in mass bands, as suggested by dual models.

Data on $\gamma_{r,v}pN^*$ photo-/electrocouplings and the related electromagnetic transition form factors [11, 12] provide important information on hadron dynamics. Decay and scattering processes require a description of hadrons in motion. This may be accomplished using Light-Front (LF) wave functions. Contributions of higher Fock states beyond $|qqq\rangle$ constituent quarks necessarily exist for relativistic dynamics. Such contributions have been modeled as $|qqq\,q\bar{q}\rangle$, $|qqq\,g\rangle$, and as meson-baryon states $|MB\rangle$.

Comparisons between models and form factor data in-

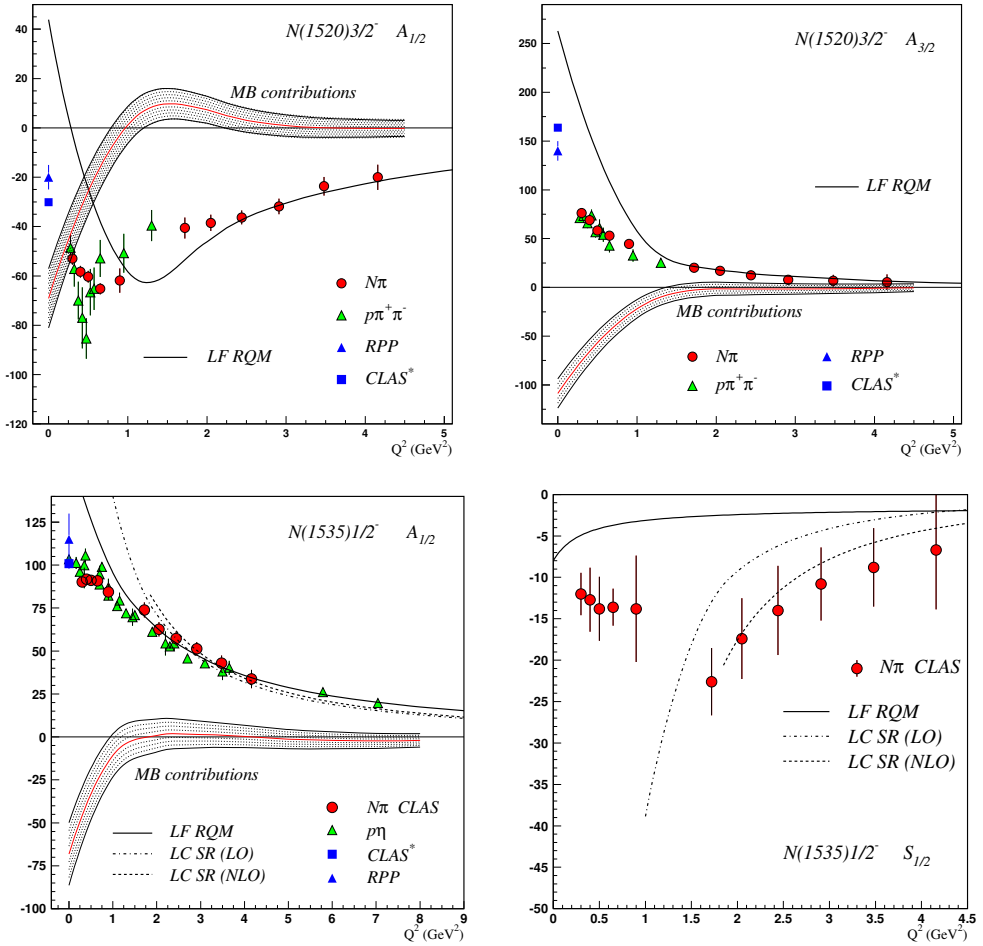

FIG. 2. Description of CLAS results on electrocouplings of the orbital-excited N(1520)3/2$^-$ and N(1535)1/2$^-$ resonance states [14–16] within a light-front quark model [25] (solid lines). The results from a light-cone sum-rule approach [26, 27] for the N(1535)1/2$^-$ electrocouplings are shown by the dotted and dash-dotted lines.

dicate that the higher meson-baryon Fock states contribute mainly at $Q^2 \lesssim 1$ GeV^2, whereas "constituent quark core" $|qqq\rangle$ configurations start to dominate at higher $Q^2 \gtrsim 2.0$ GeV^2. This is consistent with dimensional counting rules.

Light-Front quantization provides a frame-independent formalism for hadron dynamics and structure. Models can be constructed such that a mass scale that emerges from the equations of motion, leading to a specific confinement potential. Such an outcome is achieved using a LF holography approach based on the duality between the front form and AdS$_5$, the space of isometries of the conformal group. The predictions for the meson and baryon spectra are in general agreement with experimental observations and have some similarities with Dyson-Schwinger equation (DSE) analyses that describe baryons as dynamical bound states of a quark and a composite diquark [32, 33]. This LF approach has the potential to predict the Q^2-evolution of the $\gamma_v pN^*$ electrocouplings over the full resonance spectrum.

The CLAS results on $\gamma_v pN^*$ electrocouplings initiated new developments in Light-Front relativistic quark models (LF RQM) by implementing a momentum dependent quark mass inferred from DSE and lQCD approaches and accounting for the contributions of both inner quark core and outer meson-baryon cloud effects [25, 34]. This model describes successfully nucleon electromagnetic form factors at $Q^2 < 20$ GeV^2 and electroexcitations of several resonances $\Delta(1232)\frac{3}{2}^+$, $N(1440)\frac{1}{2}^+$, $N(1520)\frac{3}{2}^-$, and $N(1535)\frac{1}{2}^-$ at $Q^2 < 5$ GeV^2, see e.g. Fig. 2. Predictions on resonance electroexcitation amplitudes at 5 GeV^2 $< Q^2 <$ 12 GeV^2 are readily available. At $Q^2 > 2.0$ GeV^2 the results from the LF RQM and DSE approaches on $N \to N(1440)1/2^+$ electrocouplings are almost identical and describe the CLAS results well, see Fig. 1, further supporting the claim to access the dressed quark mass function from the experimental data on $\gamma_v pN^*$ electrocouplings.

Electroexcitation amplitudes for most N^*, Δ^*-states in the mass range M < 2.0 GeV were evaluated within the framework of a hypercentral Constituent Quark Model (hCQM) at $Q^2 < 5.0$ GeV^2. The hCQM wave functions have been adjusted to reproduce the N^* spectrum, so

that all calculations of the $\gamma_v pN^*$ electrocouplings are parameter free [35]. The electrocoupling behavior at $Q^2 > 1.0$ GeV^2 is generally well reproduced, while some lack of predicted strength at $Q^2 < 1.0$ GeV^2 is evident, where the meson-baryon cloud contributions are maximal. A relativised hCQM versio, whch incorporates quark-antiquark pair production mechanisms, and an extension of the resonance electrocoupling calculations into the Q^2-range from 5.0 GeV^2 to 12 GeV^2 are in preparation.

Relativistic quark models in an Effective Field Theory (EFT) approaches extend the capability to describe the resonance spectrum and the $\gamma_{r,v}pN^*$ photo-/electrocouplings based on QCD related model ingredients. They currently provided a reasonable description of the N* spectrum as well as the elastic nucleon and $N \to N(1440)1/2^+$ transition form factors [33, 36]. EFT approaches are promising in particular for comprehensive studies of the hybrid baryon spectrum and its electroexcitation amplitudes. These efforts are in progress.

Charmonium decays to N^*'s are timelike analogues of the spacelike form factors discussed so far because the charm quark annihilation provides a nearly pointlike ($|ggg\rangle$) current. The remarkable differences between the J/ψ and ψ' decay patterns might indicate that the ψ' state has a significant $c\bar{c}\,q\bar{q}$ Fock component.

Duality is a pervasive feature of hadron data but remains poorly understood. It suggests that the couplings of N^*'s with different spins but similar masses are correlated, so as to build up scattering amplitudes with Regge behavior at high energies. This is expressed in terms of Finite Energy Sum Rules, based on analyticity and Regge exchange.

A photon of virtuality Q^2 couples coherently to the charge at impact parameters $b \lesssim 1/Q$. The dependence of the b-distribution on the final state in processes such as $eN \to e\,\pi N$, $eN \to e\,\bar{K}\Lambda$, ... gives information on the transverse size of the relevant Fock states. This is complementary to studies of color transparency.

B. Challenges

Hadrons are bound states generated by QCD. Just like QED atoms and even single electrons or photons, hadrons are infinitely complex. Data on the hadron spectrum and scattering reveals unexpected regularities and apparent simplicities that provide clues to approximation schemes.

Computations of $\gamma_v pN^*$ electrocouplings for the full resonance spectrum and in a wide range of photon virtualities $Q^2 < 12$ GeV^2 within different quark model approaches underlines the importance of the experimental N* program with the CLAS/CLAS12 detectors at JLab. The detailed comparison of the available CLAS and foreseen from the CLAS12 results on $\gamma_v pN^*$ electrocouplings with the predictions from different model approaches will offer an excellent opportunity to refine the models and their ingredients. Consistent results on resonance electrocouplings based on QCD approaches such as DSE, lQCD, and quark models, supported by the experimental data on resonance electrocouplings, will independently validate credible access to strong interaction dynamics. Modeling of the hybrid baryon spectrum and electrocouplings, at least at $Q^2 < 2.0$ GeV^2, is of particular importance in the planned search for new states of baryon matter with the CLAS12 detector.

Relativistic covariance is required to describe scattering processes. It has been incorporated, at least approximately, in LF models discussed at this meeting. Scattering amplitudes are analytic functions. This allows to relate their real and imaginary parts via dispersion relations. Analyticity, together with duality, provides constraints in the form of Finite Energy Sum Rules. Their incorporation in fits to data could potentially reduce the ambiguities in the baryon spectrum in current models.

Unitarity at the hadron level provides a challenge for quark models, which generally do not predict couplings between hadrons. Contributions of higher Fock states may be described either in the quark-gluon ($|qqq\,q\bar{q}\rangle$, $|qqq\,g\rangle$, ...) or hadron ($|MB\rangle$, ...) bases. Each basis is presumably complete, so $|qqq\,q\bar{q}\rangle + |MB\rangle$ must be handled with care in order to avoid issues of over-counting. A complementarity between the hadron and quark bases is observed in the data and called "duality", but its origins remains unclear.

Hadron dynamics is qualitatively novel and presents a tremendous challenge. Fortunately, the underlying theory of QCD is known. High precision experiments coupled with sophisticated data analyses, lattice calculations, and advanced modeling provide an opportunity to relate observations and strong QCD to the fundamental theory.

Presentations: Inna Aznauryan, Stanley J. Brodsky, V. Burkert, Paul Hoyer, Valery Lyubovitskij, Vincent Mathieu, Igor T. Obukhovsky, Elena Santopinto, Adam P. Szczepaniak, and Bing-Song Zou.

III. DYSON-SCHWINGER EQUATIONS

A theoretical understanding of the spectrum and structure of light baryons continues to pose an exciting and challenging problem in light of new advances with photo- and electroproduction experiments [4, 11, 12, 14–16, 18, 37, 38]. In recent years steady progress has been made in combining Dyson-Schwinger equations and covariant Bethe-Salpeter and Faddeev equations [39–44]. Their central feature is that they allow us to connect experimentally based hadron parameters, such as spectra, elastic and transition form factors, and partonic structure functions, with the underlying properties of QCD's n-point functions, such as dressed quark and gluon propagators, their three- and four-point functions, etc. These quantities encode, for example, the role of dynamical chiral symmetry breaking in the generation of

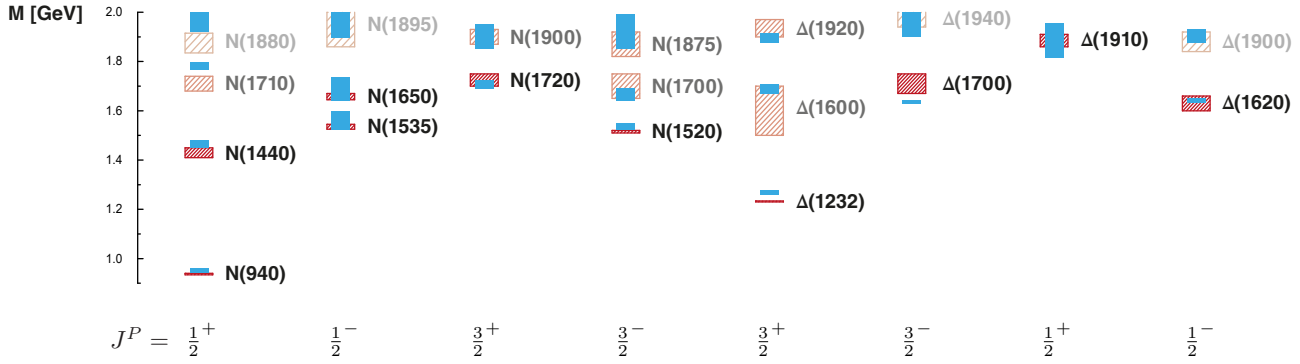

FIG. 3. Light baryon spectrum in a quark-diquark approach with reduced pseudoscalar and vector diquarks [39]. The calculated masses (solid boxes, blue) are compared to the experimental spectrum (hatched boxes, red).

hadron masses, the nature of quark-gluon confinement,[1] the connection between spacelike and timelike properties of hadronic form factors, and the microscopic origin of meson-cloud effects that dress a hadron's "quark core" to generate the rich dynamical features of hadronic scattering amplitudes that are measured experimentally. Although the complexity of the problem is still a limiting factor in practical applications and truncations, the DSE approach has matured to a point where a simultaneous description of meson and baryon properties has become feasible, which enables predictions that can be tested in ongoing and future experiments.

A paradigmatic example is given by the "missing resonances" in the baryon spectrum which, despite predictions from the quark model, have not been observed in πN scattering experiments, thus suggesting the possibility of diquark correlations or spatially-extended diquark-quark configurations in the structure of nucleon resonances. Indeed, the solution of the three-body Faddeev equation [39, 45] reveals that two quarks prefer to cluster in a color-antitriplet diquark configuration inside baryons generating non-pointlike dynamical diquark, which allows one to simplify the three-body problem to a quark-diquark system [46, 47]. New results from photo- and electroproduction experiments have ruled out early pointlike diquark models. Still, a contact-interaction treatment can reproduce the features of the low-lying spectrum [48], and sophisticated approaches using non-pointlike diquarks produce a rich phenomenology that provides insight in the underlying dynamics of baryons. Figure 3 shows the resulting baryon spectrum [39], where the quarks and diquarks are calculated from their Dyson-Schwinger and Bethe-Salpeter equations. It turns out that the lowest-lying scalar and axialvector diquarks remain the dominant components for all states. The corresponding orbital angular momentum decomposition [49] underlines the fact that baryons carry all possible values of L due to Poincaré invariance: although they exhibit clear traces of the non-relativistic quark model, already the nucleon and Δ have sizable $L = 1$ components in their rest frames.

More information about the structure of the nucleon and its resonances is encoded in their form factors. Results for the nucleon's elastic form factors show a remarkable agreement with experiment both in the quark-diquark and three-quark Faddeev approaches [50, 51]. The main discrepancies appear at low Q^2 and signal the absence of meson-baryon dynamics, which would produce characteristic non-analyticities in the timelike region and in the chiral limit of vanishing current-quark masses. At moderate spacelike Q^2, however, the meson cloud fades away and reveals the "quark core" of the baryon. This is also the transition point where currently available Dyson-Schwinger calculations can provide quantitative predictions on top of qualitative insight: as for example, that scalar-diquark dominance leads to a suppression of the d-quark compared to the u-quark contributions to form factors [52] and that orbital angular momentum due to dressed quarks is shaping the Q^2 evolution of elastic form factors and the G_E^p/G_M^p ratio [53] as well as the $\gamma^* N \to \Delta$ transition form factors [41, 51, 54, 56].

The experimental results from CLAS [14, 16] on the $N \to \Delta$ and $N \to N(1440)1/2^+$ transition form factors, which have been studied using DSEs [17, 41, 55, 56], have for the first time confirmed the DSE expectation of a dynamically running mass for dressed light quarks. The DSE evaluations with fixed quark mass fail in describing the aforementioned transition form factors at $Q^2 > 3.0$ GeV^2. In this range of photon virtualities the discrepancies between the experimental results and DSE expectations increase with Q^2. Instead, employing the dynamical running quark mass as inferred from DSE al-

[1] Confinement remains a very open question. In fact, there is no agreed definition. In this section, confinement is understood to be connected with dramatic, dynamically-driven changes in the analytic structure of QCD's propagators and vertices, which lead colored n-point functions to violate the axiom of reflection positivity and hence forces elimination of the associated excitations from the Hilbert space associated with asymptotic states. This is certainly a sufficient condition for confinement. Details can be traced from Ref. [44].

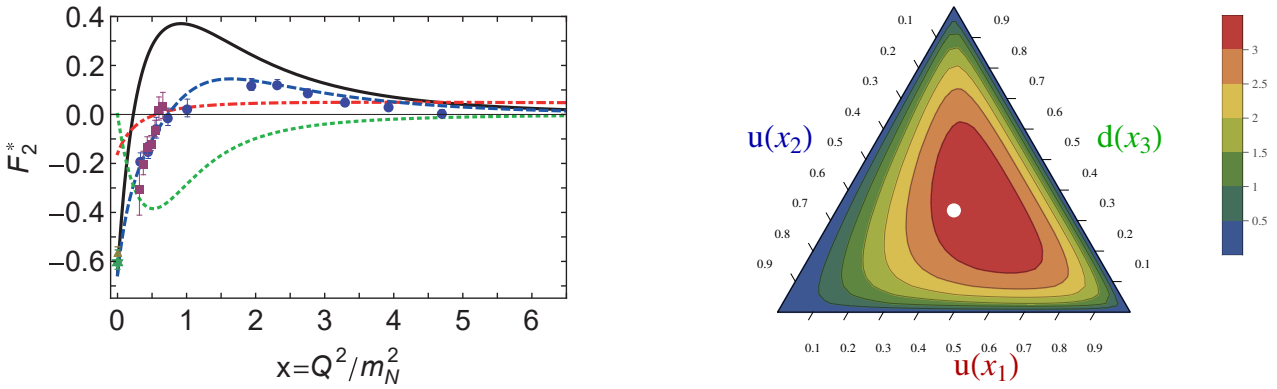

FIG. 4. *Left:* Q^2 evolution of the Pauli-like nucleon-to-Roper transition form factor. The data points from CLAS [14–16] are shown as filled circles. The solid (black) curve is the calculated result; the remaining curves are explained in [17]. *Right:* Barycentric plot of a leading-twist parton distribution amplitude $\varphi(x_1, x_2, x_3)$ for a proton containing both scalar and axialvector diquark correlations [59].

lows for a good description of the measured nucleon elastic and transition form factors in the Q^2-range where quark core contributions dominate ($Q^2 > 2.0$ GeV^2). This successful description of nucleon elastic form factors and the electroexcitation amplitudes of the $\Delta(1232)3/2^+$ and $N(1440)1/2^+$ resonances with distinctively different structure achieved with the same dressed quark mass function clearly demonstrates the relevance of dressed quarks as ground and excited nucleon structural components and the capability of DSE to access the dressed quark mass function from the combined analysis of the experimental results on elastic and transition form factors.

Currently DSEs provide the only approach with the capacity to compute dressed quark core contribution to the resonance electroexcitation amplitudes starting from the QCD Lagrangian. Figure 4 shows the nucleon-to-Roper transition form factor $F_2^*(Q^2)$ [17], which exhibits the characteristic zero crossing pertinent to the nature of the Roper as a radial excitation. The DSE calculation is in good agreement with the experimental results where the meson-baryon contributions are diminished. Moreover, the DSE results [17] are also consistent with the results from a recent LF quark model study with momentum-dependent constituent quark mass [25, 34]. These findings support the emerging consensus that the Roper is indeed the first radial excitation of the nucleon, and a flavor analysis uncovers a scalar-diquark dominance and d-quark suppression that resembles the situation in the nucleon elastic form factors [57]. The observed differences between the experimental results and DSE expectation at $Q^2 < 1.0$ GeV^2 indicates the importance of meson-baryon dressing effects, which are significant or even dominant at the distances comparable with baryon sizes where the internal composition of the state is quite different from the pure quark core contribution expectation. Sizable meson-baryon cloud contributions masked for a long time the quark structure of the Roper. Dyson-Schwinger studies of other nucleon-to-resonance transition form factors have only begun and many more results are expected in upcoming years.

Another promising avenue to expose the underlying diquark structure of baryons is to investigate parton distribution amplitudes (PDAs), where recent progress in the meson sector [58] has paved the way to similar studies for the nucleon and the Roper resonance. Figure 4 shows the nucleon PDA within a dynamical diquark-quark approximation, which is consistent with computations in lattice QCD [60]. In the near future these investigations will be extended to nucleon electromagnetic form factors and resonance electroexcitation amplitudes at large momentum transfer, which will allows us to further test factorization at the distances where the transition from strong to perturbative QCD takes place. Similarly to the case of the pion [61], this also provides the first step toward accessing other non-perturbative structure properties, including PDFs and GPDs.

Naturally, a detailed understanding of baryon properties requires simultaneous efforts in constructing Bethe-Salpeter kernels beyond the leading rainbow-ladder truncation. By analyzing the symmetries of QCD and solving the corresponding Ward-Green-Takahashi identities, the quark-gluon vertex and two-body scattering kernel can be constructed accordingly. The resulting truncation is capable of describing the light hadron spectrum including ground and low-lying radially excited states and is also applicable for hadron structure studies [62, 63]. These advances are complemented, *e.g.*, by further investigations of the quark-gluon vertex [64–68], the inclusion of pion-cloud effects in the baryon spectrum [69], and the application of n-particle irreducible methods in the systematic construction of Bethe-Salpeter kernels together with QCD n-point functions [39, 70]. Eventually, the progress made in these areas will help to bridge the gap between our present understanding of the nucleon's "quark core" and the wealth of phenomena that consti-

tutes the spectrum and structure of excited nucleons in QCD.

Presentations: Adnan Bashir, Chen Chen, Ian Cloët, Gernot Eichmann, Bruno El-Bennich, Cédric Mezrag, Sixue Qin, and Jorge Segovia.

IV. LATTICE QCD

Nucleon excitations emerge as dynamical enhancements in baryon-meson scattering and photo- and electroproduction cross sections. In order to connect the N^* spectrum with the fundamental theory of strong interactions, QCD, one needs a non-perturbative tool that allows for the study of these cross sections and from them the access to properties of their resonant content. Lattice gauge calculations enable a numerical solution of QCD, where all quark and gluonic contributions are non-perturbatively included. Being exact in QCD dynamics, it includes the so-called "quark-core" and "pion-cloud" effects. More generally, all multi-body effects are included exactly with only systematically-improvable approximations that will be discussed below. As a result, lattice QCD is in principle a tool that allows for the determination of resonant, as well as non-resonant, scattering amplitudes without the need for uncontrolled approximations. There are at least two reasons for having a theoretical QCD program running in parallel with the experimental program. First, it will guide and confirm experiments as they consider increasingly complex reactions. Second, it will allow for the determination of experimentally inaccessible quantities (e.g., elastic form factors of exotic states) that will shed further light onto the nature of these states.

The study of resonance properties, including the hybrid and non-hybrid N^* spectrum, relies on formal and technical advances that are presently being developed and tested in benchmark calculations, some of which were highlighted at this workshop. To understand these, a brief summary of the building blocks of lattice QCD calculations is given. In order to obtain exact QCD quantities, correlation functions are evaluated using the path integral formalism. Path integrals can be statistically determined using Monte Carlo sampling. In order to assure a positive definite measure, one must analytically continue time so that spacetime has a Euclidean signature. In order to evaluate correlations functions numerically, it is necessary to discretize and truncate spacetime. This introduces UV and IR cutoffs. The only parameters one can tune in a lattice QCD calculation are the bare masses of the dynamical quarks and the quark-gluon coupling. One can recover QCD observables from their lattice QCD counterparts by taking the limit where these cutoffs are removed and the quark masses correspond to the physical ones. For a recent review on lattice QCD see [5]. In the determination of scattering amplitudes, the truncation of spacetime plays a crucial role which we briefly discuss.

Presently, the most reliable observable obtained from lattice QCD is the finite-volume energy spectrum. Accurate and precise determination of this has been made possible by the development of numerical techniques such as "distillation" [71] and "variational method" [72–74]. This is exemplified by the results presented in Fig. 5 from the Hadron Spectrum Collaboration [31]. In this exploratory calculation, the excited N^* and Δ^* spectrum is determined for the first time. This calculation was performed using unphysically heavy quark masses corresponding to $m_\pi = 391$ MeV, which partly explains any discrepancy with the experimentally observed spectrum. One crucial approximation performed in this study is the fact that the resonant nature of the states beyond the lowest-lying $N^{1/2+}$ and $\Delta^{3/2+}$ has been ignored. This is highlighted by the fact that most of the energy levels lie above a multitude of open thresholds. In the figure we depict only the pion production thresholds as open circles on the rightmost axis.

The field is now focused on removing this approximation. For the study of resonances that couple to two-body states, it is formally understood how to extract resonant as well as non-resonant scattering amplitudes from the finite-volume spectrum [82, 83]. So far, these ideas have been primarily implemented in the mesonic sector. Two prominent examples of this include the isoscalar [75] and isovector [76] $\pi\pi$ scattering amplitudes, shown in Fig. 6. Just as in most experimental analyses, lQCD constrains amplitudes to real energy values on the physical Riemann sheet. Meanwhile, resonances correspond to complex poles on unphysical sheets. By performing fits to the scattering amplitudes obtained via lQCD, and assuming some parametrization, one can deduce the resonance poles. From the real and imaginary components of the pole, one obtains the mass and width of the corresponding resonance, respectively. Figure 6 shows examples of these fits, with the pole locations shown in the lower panels. Most excitingly, these calculations are now being performed for energies where multiple channels can be kinematically open and arbitrarily coupled [84].

The isoscalar $\pi\pi$ scattering amplitude illustrates a useful theoretical capacity that can be exploited in lQCD: while experimentally the quark masses are fixed by Nature, theoretically one can vary these at will. This turns out to be very useful. For instance, one can consider the pole position of the ρ resonance as a function of the quark masses, see Fig. 6(d). What is observed, is that as the quark masses increase the phase space for the ρ to decay decreases and consequently it becomes increasingly narrow. At around $m_\pi \sim 410$ MeV the ρ becomes a stable bound state. The ρ is a fairly narrow resonance in Nature, so not much is gained from this exercise. On the other hand, the $\sigma/f_0(500)$ resonance is remarkably broad in Nature, see Fig. 6(c). This has led to a long standing controversy of its existence [78]. By increasing the quark masses to be unphysically heavy, one expects this to be increasingly narrow for reasons already mentioned, and this is indeed what is observed [75]. In fact, it is found

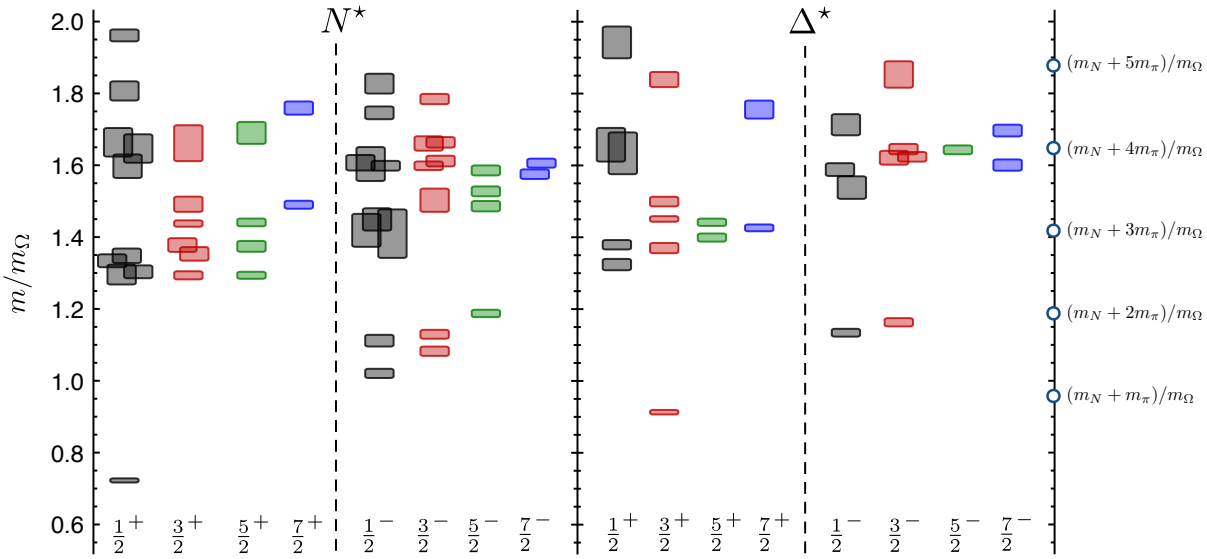

FIG. 5. Shown is the low-lying N^* and Δ^* spectrum obtained using $m_\pi = 391$ MeV [31]. Each tower of states is labeled by the corresponding J^P. On the rightmost axis, we label the thresholds where $N + n\pi$ states can go on-shell, with $n = 1 \ldots 5$.

to be bound at $m_\pi = 391$ MeV. In summary, by considering unphysically heavy quark masses one can expect to more easily find evidence of broad resonance, like the Roper. One can then proceed to continuously dial the quark masses to their physical values and observe the trajectory of the poles as a function of the parameters of the Standard Model.

Determining the mass and width of the hadronic resonance is one goal of the program for studying resonances from lQCD, but this program will also allow for the determination of experimentally inaccessible observables. One important example of these is the elastic form factors of resonances [85], which have often been the subject of model studies for similar reasons. This is a fairly new idea in lQCD that is still being developed and stems from the notion of extracting transition form factors for processes where a resonance is present in the initial or final state [86]. This method has recently been demonstrated in the first determination of a resonance form factor from lattice QCD [87]. The method for accessing the elastic form factors of resonances will partly capitalize on the ongoing efforts to obtain the form factors of, for example, the nucleon [88], but they differ from these in conceptually important ways. What one can access directly from lQCD is the scattering amplitude involving an external current evaluated for real-valued energies [85]. From this amplitude, one can access the form factor of a resonance, by analytically continuing this amplitude to its resonant pole and extracting the residue, which can then be related to its form factor. This is the procedure that was followed in [87] to extract the $\rho \to \pi\gamma^*$ form factor.

Presently, one of the largest limitations for the proposed program is the fact that a good number of hadronic resonances lie above thresholds where three or more particles can go on-shell. For example, the Roper lies above the $N\pi\pi$ threshold and it decays to this state approximately 25%-50% of the time. Therefore, one cannot ignore the mixing between $N\pi$ and $N\pi\pi$ in this channel without violating unitarity. Being exact in the QCD dynamics, lattice states above the $N\pi\pi$ threshold will necessarily obtain information about both two- and three-body states. Understanding how this information is embedded inside finite-volume states is an ongoing field of research [89]. Most recently, a relationship was obtained between finite-volume states and scattering amplitudes for theories where two- and three-body states can be arbitrarily coupled [90]. Although a universal relation between finite-volume and infinite-volume states above the three-particle threshold is currently lacking, we suspect such an equation will be derived in the future and subsequent lQCD calculation of three-body scattering amplitudes will be performed.

The practical application of these ideas is more challenging in the baryon sector than in the meson sector for several reasons. Firstly, baryons in lQCD suffer from smaller signal-to-noise ratios than mesons. Secondly, the complexity and hence computational cost is increased due to the larger number of quarks/antiquarks in baryons as compared to mesons. Thirdly, there is typically a larger number of open channels of different flavor combinations in the baryon sector than in the meson sector. Finally, the partial-wave formulation is somewhat more complicated owing to the spin of the baryons. Nevertheless, the underlying theoretical and computational developments are now in place, and the practical extension to baryons needs only increasing computational power and the experience gained in the meson sector.

In summary, lQCD has proven to be a powerful tool

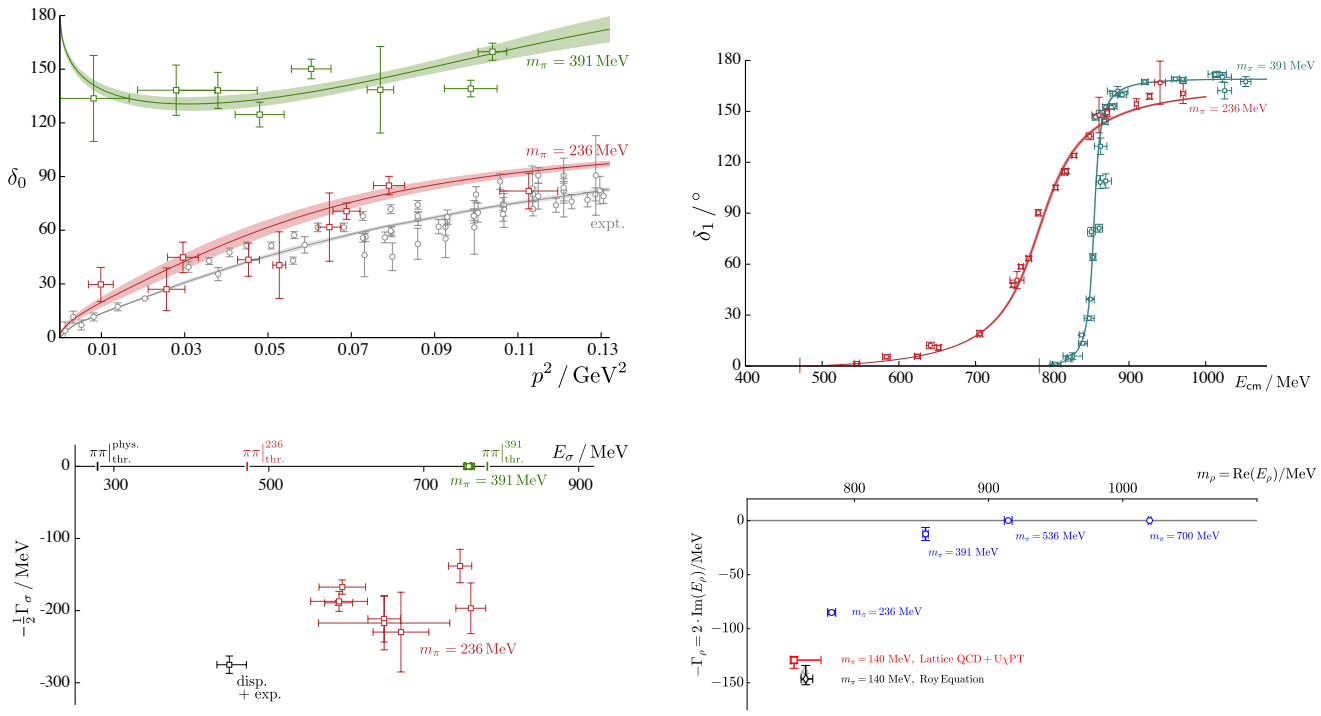

FIG. 6. We show the (a) isoscalar [75] and (b) isovector [76] $\pi\pi$ scattering phase shifts obtained using $m_\pi = 236, 391$ MeV. The experimental points are from [77]. We also show the mass and width of the (c) σ [75, 78–80] and (d) ρ [76, 79, 81] resonances for a range of values of m_π including the experimental point.

in the determination of hadronic properties. The field has primarily been focused on the study of QCD-stable states, since these are technically and conceptually simpler, but we have witnessed a great deal of progress in the utilization of this tool for the study of QCD-unstable states. Although the formal developments are universal, the exploratory calculations have been performed in the mesonic sector, for a variety of reasons. It is natural to expect that analogous calculations in the baryonic sector will soon be performed. In order to study increasingly complex systems, such as the Roper and other interesting states, further theoretical development is currently under way. We envision lQCD will grow to provide reliable determinations of various properties of these states, including experimentally inaccessible observables that will assist in understanding their nature.

Presentations: Raul Briceño and David Richards.

V. REACTION THEORY

To establish a coherent picture of nucleon resonances, analyses from complimentary approaches using a variety of tools are important. In this workshop, progress from ANL-Osaka, Bonn-Gatchina (BoGa), Jülich-Bonn (JuBo), and SAID was reported on the analysis of meso-, photo-, and electroinduced meson-production reactions.

In the ANL-Osaka approach, nucleon resonances up to an invariant mass $W = 2$ GeV have been investigated within a dynamical coupled-channel (DCC) model of πN and γ-proton reactions [91]. The model has recently been extended to the γ-neutron reaction to disentangle the isospin structure of the photoexcitation couplings of $I = 1/2$ N^* resonances [92] and to the neutrino reaction [93], where the electromagnetic transition form factors and axial-vector couplings of N^* are studied. In this workshop, preliminary results on the $N \to N^*$ electromagnetic transition form factors were reported for $\Delta(1232)3/2^+$, $N(1440)1/2^+$, $N(1520)3/2^-$, and $N(1535)1/2^-$, which are extracted by analyzing the data in single-pion electroproduction reactions off the proton up to $Q^2 = 6$ GeV^2 from CLAS. In this study, the transition form factors are defined with the residue of the resonance pole. This inevitably makes them complex, which is associated with the essential nature of the resonances as decaying particles.

The model dependence of meson loops on the $N \to N^*$ transition form factors was also discussed by comparing the form factors obtained from different dynamical models that contain a different number of reaction channels and bare N^* states. The magnitude of the πN-loop contribution is found to be stable within the various models. However, the loop contribution from unstable particle channels, such as $\pi\Delta$ and σN, is found to vary significantly over the models. This implies that an extension of

the analysis that includes the two-pion production data is necessary. Such an extensive analysis including the two-pion production data is planned to be performed.

The $\pi^+\pi^- p$ electroproduction off protons amplitudes were determined from the fit of the CLAS $\pi^+\pi^- p$ electroproduction cross sections [94, 95] within the framework of a single-channel meson-baryon reaction model JM [15, 16, 96] at $Q^2 < 1.5$ GeV^2. They offer valuable input to be incorporated to the multi-channel global analysis of exclusive meson electroproduction in the resonance excitation region. In this regard, the new measurement of the $(\pi, 2\pi)$ reaction in the scheduled experiment at J-PARC, the J-PARC E45 experiment, will also be very helpful to obtain more information on nucleon resonances with a large branching ratio to $\pi\pi N$.

The combined analysis of the data from reactions with two and three particles in the final state is one of the main strengths of the Bonn-Gatchina (BoGa) coupled-channel approach [97]. Most resonances with masses above 1.8 GeV have a rather small πN coupling and are observed either in final states with open strangeness [98] or in reactions with two final-state mesons [99]. In the case of three-particle final states, the data are analyzed exploiting a maximum likelihood method, which takes all correlations in the multi-dimensional phase volume into account. The combined analysis of the data obtained from all measured final states provides a possibility to define uniquely the structure of the partial wave amplitudes and to define all decay couplings as pole residues of the observed states. In the analysis, both meso- and photoinduced, and reactions off proton and neutron targets are included. Thus the γ-proton and γ-neutron couplings of baryon resonances can be defined accurately [100]. In this workshop, BoGa results on new unpolarized and polarized data in two-pion final states were presented. In the near future, the BoGa approach will be expanded to include analyses of meson electro- and dilepton production reactions. This will provide an opportunity to extract the form factors of baryon resonances in the time- and space-like regions.

The Jülich-Bonn (JuBo) approach represents another dynamical coupled-channel model for the study of meso- and photoinduced reactions [101]. As in the other two discussed DCC approaches, resonances are defined as poles in the complex plane with their residues representing branching fractions into the different channels γN, πN, $\pi\Delta$, σN, ρN, and KY (same channels as the ANL-Osaka approach). The analysis of kaon photoproduction is finished and was presented at the workshop.

As for pion electroproduction, the SAID group has performed fits that have incorporated all available $N\pi$ electroproduction data simultaneously with the photoproduction data that provides the real-photon limit. The Q^2 evolution of multipoles has so far only been published online [102]. The discussed redefinition of helicity couplings at the pole and their Q^2 dependence, based on SAID and MAID fits, has recently been achieved for the $\Delta(1232)3/2^+$ [103] and will be extended to other resonances.

As data in photoproduction reactions are produced at unprecedented accuracy, and for more and more polarization observables and final states, analysis tools are developing accordingly to provide statistically more rigorous evidence of resonances and their properties. One step in this direction is given by statistically meaningful single-energy solutions of elastic πN scattering that can be used in multi-channel analyses by other groups to make them entirely driven by data [104]. Another question is which terms, in particular resonance terms, are needed in the parametrization of the reaction amplitudes. This can be systematically studied using model selection techniques [105].

Presentations: Michael Döring, Hiroyuki Kamano, Deborah Rönchen, Andrey Sarantsev, and Toru Sato.

VI. FUTURE

CLAS12 is the only facility foreseen worldwide that will be able to search for hybrid baryons in electroproduction processes and, in providing access to an enormous range of final-state baryon quantum numbers with electro-production transitions at up to $Q^2 \sim 12\,\text{GeV}^2$, it is uniquely capable of exposing many facets of the transition between the strong and perturbative domains of QCD. It follows that the associated experimental and theoretical programs, working together, will supply crucial insights concerning some of the most pressing questions in modern science, viz. what is the origin of more than 98% of visible mass in the Universe, how is that source connected with confinement, and how do both emerge from the Standard Model? In discussing these issues, a *plan of action* was developed by the participants, some items in which are listed here:

- Develop a synergistic experiment-theory effort aimed at charting and understanding the Q^2-dependence of N^* structure, with particular emphasis on the transition from infrared momenta, where meson-baryon final-state-interactions (MB-FSIs) are important, to the domain of dominance by the dressed-quark core.

- Secure theory support for completion of studies of the N^* spectrum in the mass range above 1.8 GeV via a combined multi-channel analysis of data on exclusive meson photo- and electroproduction from the nucleon, including both differential cross-sections and a variety of polarization asymmetries.

- Develop reaction models which respect first-principles constraints on amplitudes, such as unitarity, analyticity and crossing symmetry, for the extraction of resonance properties from experimental data or lQCD simulations at finite volume; and

models that explicitly and meaningfully incorporate quark degrees-of-freedom in the description of the non-resonant components of electro-production amplitudes, a feature that is crucial both for understanding CLAS12 data on $Q^2 > 5\,\mathrm{GeV}^2$ and for GPD and TMD extractions.

- Develop reliable methods for the description of three-particle production reactions, e.g. $\pi\pi N$, and their role in the formation of excited baryons.

- Develop methods required for identification of hybrid baryon states in analyses of data on $N\pi$, $N\pi\pi$ and KY exclusive electro-production off protons using the CLAS12 detector, with particular emphasis on those techniques which can distinguish between bound-quark and open-channel MB-FSI effects.

- Continue experimental analyses of $N\pi$, $N\pi\pi$ and KY exclusive meson electro-production data from CLAS, extending existing information on the Q^2-dependence of $\gamma_v NN^*$ electro-couplings to resonances in the mass range above 1.6 GeV; and initiate experimental studies of resonance electro-excitation from bound nucleons.

- Continue development of both improved truncation schemes for theoretical approaches to continuum-QCD and sound phenomenological models. Extend the calculation of electroexcitation amplitudes to nucleon resonances with distinctively different structure in the full range of photon virtualities $Q^2 < 12\,\mathrm{GeV}^2$ accessible in experiments planned with CLAS12. Refine methods for relating data on the Q^2-evolution of resonance electrocouplings to the running coupling and masses in QCD, and therefrom develop insights into the mechanism behind hadron mass generation and its many corollaries.

- Pursue lQCD extraction of the N^* spectrum via analytical continuation of the scattering amplitude from the real-axis, discrete lQCD energy spectrum to the complex plane, where resonance poles lie; and develop reliable methods for computation of electromagnetic nucleon-to-resonance transition amplitudes on the domain of experimentally accessible virtualities.

- Work toward the computation of excited nucleon properties, including generalized parton distributions and transverse momentum dependent distributions.

Acknowledgments: Research supported by U.S. Department of Energy (DOE), Office of Science, Office of Nuclear Physics, contract no. DE-AC02-06CH11357 and in parts by the U.S. National Science Foundation (NSF); Alexander von Humboldt Foundation; Argonne National Laboratory, Office of the Director, through the Named Postdoctoral Fellowship Program; CIC (UMSNH) and CONACyT Grant nos. 4.10 and CB-2014-22117; CNPq nos. 305852/2014-0 and 458371/2014-9; DFG Project No. FI 970/11-1; DFG collaborative research center TR 16; Fundação de Amparo à Pesquisa do Estado de São Paulo - FAPESP Grant Nos. 2015/21550-4 and 2016/03154-7.

[1] V.D. Burkert, Few Body Syst. **57**, 873 (2016).
[2] V.D. Burkert, EPJ Web Conf. **134**, 01001 (2017).
[3] A.V. Anisovich, R. Beck, V. Burkert, *et al.*, Eur. Phys. J. A **50**, 129 (2014).
[4] V. Crede and W. Roberts, Rep. Prog. Phys. **76**, 076301 (2013).
[5] C. Patrignani *et al.*, Chin. Phys. C **40**, 100001 (2016).
[6] V. Sokhoyan *et al.* (CBELSA/TAPS Collaboration), Eur. Phys. J. A **51**, 95 (2015).
[7] J. Hartmann *et al.* (CBELSA/TAPS Collaboration), Phys. Lett. B **748**, 212 (2015).
[8] V. Sokhoyan *et al.* (CBELSA/TAPS Collaboration), Phys. Lett. B **746**, 127 (2015).
[9] E. Gutz *et al.* (CBELSA/TAPS Collaboration), Eur. Phys. J. A **50**, 74 (2014).
[10] I. Jaegle *et al.* (CBELSA/TAPS Collaboration), Eur. Phys. J. A **47**, 89 (2011).
[11] I.G. Aznauryan and V.D. Burkert, Prog. Part. Nucl. Phys. **67**, 1 (2012).
[12] I.G. Aznauryan *et al.*, Int. J. Mod. Phys. E **22**, 1330015 (2013).
[13] R.W. Gothe and Y. Tian, Few Body Syst. **57**, 917 (2016).
[14] I.G. Aznauryan *et al.* (CLAS Collaboration), Phys. Rev. C **80**, 055203 (2009).
[15] V.I. Mokeev *et al.* (CLAS Collaboration), Phys. Rev. C **86**, 055203 (2012).
[16] V.I. Mokeev *et al.*, Phys. Rev. C **93**, 054016 (2016).
[17] J. Segovia *et al.*, Phys. Rev. Lett. **115**, 171801 (2015).
[18] K. Park *et al.* (CLAS Collaboration), Phys. Rev. C **91**, 045203 (2015).
[19] Yu.A. Skorodumina *et al.*, Bull. Russ. Acad. Sci. Phys. **79**, 532 (2015).
[20] H. Denizli *et al.* (CLAS Collaboration), Phys. Rev. C **76**, 015204 (2007).
[21] V.I. Mokeev, Few Body Syst. **57**, 909 (2016).
[22] R.W. Gothe, V.I. Mokeev, V.D. Burkert, P.Cole, K.Joo, and P. Stoler, Nucleon Resonance Studies with CLAS12, Experiment E12-09-003.
[23] D.S. Carman, R.W. Gothe, and V.I. Mokeev, Exclusive $N^* \to KY$ Studies with CLAS12, Experiment E12-06-108A.
[24] D.S. Carman, R.W. Gothe, and V.I. Mokeev, Nucleon Resonance Structure Studies Via Exclusive KY Electroproduction at 6.6 GeV and 8.8 GeV, Experiment E12-16-010A.

[25] I.G. Aznauryan and V.D. Burkert, Phys. Rev. C **85**, 055202 (2012).
[26] I.V. Anikin, V.M. Braun, and N. Offen, Phys. Rev. D **92**, 014018 (2015).
[27] V.M. Braun *et al.*, Phys. Rev. D **89**, 0722001 (2014).
[28] J.J. Dudek and R.G. Edwards, Phys. Rev. D **85**, 054016 (2012).
[29] Zh. Li and V.D. Burkert, Phys. Rev. D **46**, 70 (1992).
[30] A. D'Angelo, V.D. Burkert, D.S. Carman, E.N. Golovach, R.W. Gothe, and V.I. Mokeev, A Search for Hybrid Baryons in Hall B with CLAS12, Experiment E12-16-010.
[31] R.G. Edwards, J.J. Dudek, D.G. Richards, and S.J. Wallace, Phys. Rev. D **84**, 074508 (2011).
[32] G.F. de Teramond, S.J. Brodsky, A. Deur, H.G. Dosch, and R.S. Sufian, EPJ Web Conf. **137** (2017).
[33] S.J. Brodsky, G.F. de Teramond, H.G. Dosch, and C. Lorc, Int. J. Mod. Phys. A **31**, 1630029 (2016).
[34] I.G. Aznauryan and V.D. Burkert, Phys. Rev. C **92**, 015203 (2015).
[35] E. Santopinto and M.M. Giannini, Phys. Rev. C **86**, 065202 (2012).
[36] I.T. Obukhovsky *et al.*, Phys. Rev. D **89**, 0142032 (2014).
[37] E. Klempt and J.M. Richard, Rev. Mod. Phys. **82**, 1095 (2010).
[38] L. Tiator, D. Drechsel, S.S. Kamalov, and M. Vanderhaeghen, Eur. Phys. J. ST **198**, 141 (2011).
[39] G. Eichmann, H. Sanchis-Alepuz, R. Williams, R. Alkofer, and C.S. Fischer, Prog. Part. Nucl. Phys. **91**, 1 (2016).
[40] A. Bashir *et al.*, Commun. Theor. Phys. **58**, 79 (2012).
[41] C.D. Roberts, J. Phys. Conf. Ser. **630**, 012051 (2015).
[42] C.D. Roberts, J. Phys. Conf. Ser. **706**, 022003 (2016).
[43] C.D. Roberts and J. Segovia, Few Body Syst. **57**, 1067 (2016).
[44] T. Horn and C.D. Roberts, J. Phys. G. **43**, 073001/1 (2016).
[45] G. Eichmann, R. Alkofer, A. Krassnigg, and D. Nicmorus, Phys. Rev. Lett. **104**, 201601 (2010).
[46] R.T. Cahill, C.D. Roberts, and J. Praschifka, Austral. J. Phys. **42**, 129 (1989).
[47] M. Oettel, G. Hellstern, R. Alkofer, and H. Reinhardt, Phys. Rev. C **58**, 2459 (1998).
[48] C. Chen, L. Chang, C.D. Roberts, S.L. Wan, and D.J. Wilson, Few Body Syst. **53**, 293 (2012).
[49] G. Eichmann, Few-Body Syst. **58** (2017).
[50] G. Eichmann, Phys. Rev. D **84**, 014014 (2011).
[51] J. Segovia, I.C. Cloët, C.D. Roberts, and S.M. Schmidt, Few Body Syst. **55**, 1185 (2014).
[52] J. Segovia, C.D. Roberts, and S.M. Schmidt, Phys. Lett. B **750**, 100 (2015).
[53] I.C. Cloët, C.D. Roberts, and A.W. Thomas, Phys. Rev. Lett. **111**, 101803 (2013).
[54] G. Eichmann and D. Nicmorus, Phys. Rev. D **85**, 093004 (2012).
[55] D. J. Wilson, I. C. Cloet, L. Chang and C. D. Roberts, Phys. Rev. C **85**, 025205 (2012).
[56] J. Segovia, C. Chen, C.D. Roberts, and S.-L. Wan, Phys. Rev. C **88**, 032201(R) (2013).
[57] J. Segovia and C.D. Roberts, Phys. Rev. C **94**, 042201(R) (2016).
[58] L. Chang *et al.*, Phys. Rev. Lett. **110**, 132001 (2013).
[59] C. Mezrag, C. D. Roberts and J. Segovia, *in progress.*
[60] G.S. Bali *et al.*, JHEP **02**, 070 (2016).
[61] C. Mezrag, H. Moutarde, and J. Rodriguez-Quintero, Few Body Syst. **57**, 729 (2016).
[62] S.-X. Qin, Few Body Syst. **57**, 1059 (2016).
[63] S.-X. Qin, EPJ Web Conf. **113**, 05024 (2016).
[64] A. Bashir, R. Bermúdez, L. Chang, and C.D. Roberts, Phys. Rev. C **85**, 045205 (2012).
[65] E. Rojas, J.P.B.C. de Melo, B. El-Bennich, O. Oliveira, and T. Frederico, JHEP **10**, 193 (2013).
[66] A.C. Aguilar, D. Binosi, D. Ibañez, and J. Papavassiliou, Phys. Rev. D **90**, 065027 (2014).
[67] D. Binosi, L. Chang, J. Papavassiliou, S.-X. Qin, and C.D. Roberts, Phys. Rev. D **95**, 031501 (2017).
[68] R. Bermudez, L. Albino, L. X. Gutiérrez-Guerrero, M. E. Tejeda-Yeomans and A. Bashir, Phys. Rev. D **95**, no. 3, 034041 (2017).
[69] H. Sanchis-Alepuz, C.S. Fischer, and S. Kubrak, Phys. Lett. B **733**, 151 (2014).
[70] R. Williams, C.S. Fischer, and W. Heupel, Phys. Rev. D **93**, 034026 (2016).
[71] M. Peardon *et al.*, Phys. Rev. D **80**, 054506 (2009).
[72] C. Michael, Nucl. Phys. B **259**, 58 (1985).
[73] M. Luscher and U. Wolff, Nucl. Phys. B **339**, 222 (1990).
[74] B. Blossier, M. Della Morte, G. von Hippel, T. Mendes, and R. Sommer, JHEP **04**, 094 (2009).
[75] R.A. Briceno, J.J. Dudek, R.G. Edwards, and D.J. Wilson, Phys. Rev. Lett. **118**, 022002 (2017).
[76] D.J. Wilson, R.A. Briceno, J.J. Dudek, R.G. Edwards, and C.E. Thomas, Phys. Rev. D **92**, 094502 (2015).
J.J. Dudek, R.G. Edwards, and C.E. Thomas, Phys. Rev. D **87**, 034505 (2013), [Erratum: Phys. Rev. D **90**, 099902 (2014)].
[77] S.D. Protopopescu *et al.*, Phys. Rev. D **7**, 1279 (1973).
B. Hyams *et al.*, Nucl. Phys. B **64**, 134 (1973).
G. Grayer *et al.*, Nucl. Phys. B **75**, 189 (1974).
P. Estabrooks and A.D. Martin, Nucl. Phys. B **79**, 301 (1974).
[78] J. R. Pelaez, Physics Reports **658** (2016).
[79] R. Garcia-Martin, R. Kaminski, J.R. Pelaez, and J. Ruiz de Elvira, Phys. Rev. Lett. **107**, 072001 (2011).
[80] I. Caprini, G. Colangelo, and H. Leutwyler, Phys. Rev. Lett. **96**, 132001 (2006).
[81] H.-W. Lin *et al.*, Phys. Rev. D **79**, 034502 (2009).
J.J. Dudek, R.G. Edwards, P.Guo, and C.E. Thomas, Phys. Rev. D **88**, 094505 (2013).
D.R. Bolton, R.A. Briceno, and D.J. Wilson, Phys. Lett. B **757**, 50 (2016).
P. Masjuan, J. Ruiz de Elvira, and J.J. Sanz-Cillero, Phys. Rev. D **90**, 097901 (2014).
B. Ananthanarayan, G. Colangelo, J. Gasser, and H. Leutwyler, Phys. Rept. **353**, 207 (2001).
G. Colangelo, J. Gasser, and H. Leutwyler, Nucl. Phys. B **603**, 125 (2001).
Z.Y. Zhou *et al.*, JHEP **02**, 043 (2005), [hep-ph/0406271].
P. Masjuan and J.J. Sanz-Cillero, Eur. Phys. J. **C73**, 2594 (2013).

[82] M. Luscher, Commun. Math. Phys. **105**, 153 (1986).
M. Luscher, Nucl. Phys. B **354**, 531 (1991).
K. Rummukainen and S.A. Gottlieb, Nucl. Phys. B **450**, 397 (1995).
S. He, X. Feng, and C. Liu,JHEP **07**, 011 (2005).
C. Kim, C.T. Sachrajda, and S.R. Sharpe, Nucl. Phys. B **727**, 218 (2005).
N.H. Christ, C. Kim, and T. Yamazaki, Phys. Rev. D **72**, 114506 (2005).
M.T. Hansen and S.R. Sharpe, Phys. Rev. D **86**, 016007 (2012).
R.A. Briceno and Z.Davoudi, Phys. Rev. D **88**, 094507 (2013).
[83] R.A. Briceno, Phys. Rev. D **89**, 074507 (2014).
[84] G. Moir, M. Peardon, S.M. Ryan, C.E. Thomas, and D.J. Wilson, JHEP **10**, 011 (2016).
J.J. Dudek, R.G. Edwards, and D.J. Wilson, Phys. Rev. D **93**, 094506 (2016).
D.J. Wilson, J.J. Dudek, R.G. Edwards, and C.E. Thomas, Phys. Rev. D **91**, 054008 (2015).
J.J. Dudek, R.G. Edwards, C.E. Thomas, and D.J. Wilson, Phys. Rev. Lett. **113**, 182001 (2014).
[85] R.A. Briceno and M.T. Hansen, Phys. Rev. D **94**, 013008 (2016).
V. Bernard, D. Hoja, U. G. Meissner, and A. Rusetsky, JHEP **09**, 023 (2012).
[86] L. Lellouch and M. Luscher, Commun. Math. Phys. **219**, 31 (2001).
R.A. Briceno and M.T. Hansen, Phys. Rev. D **92**, 074509 (2015).
R.A. Briceno, M.T. Hansen, and A. Walker-Loud, Phys. Rev. D **91**, 034501 (2015).
[87] R.A. Briceno *et al.*, Phys. Rev. D **93**, 114508 (2016).
R.A. Briceno *et al.*, Phys. Rev. Lett. **115**, 242001 (2015).
[88] J.R. Green *et al.*, Phys. Rev. D **90**, 074507 (2014).
J. Green *et al.*, Phys. Rev. D **92**, 031501 (2015).
B. Yoon *et al.*, Phys. Rev. D **93**, 114506 (2016).
B. Yoon *et al.*, Phys. Rev. D **95**, 074508 (2017).
[89] M.T. Hansen and S.R. Sharpe, Phys. Rev. D **93**, 014506 (2016).
M.T. Hansen and S.R. Sharpe, Phys. Rev. D **93**, 096006 (2016).
K. Polejaeva and A. Rusetsky, Eur. Phys. J. A **48**, 67 (2012).
R.A. Briceno and Z. Davoudi, Phys. Rev. D **87**, 094507 (2013).
[90] R.A. Briceno, M.T. Hansen, and S.R. Sharpe, arXiv:1609.09805 [hep-lat] (2016).
[91] H. Kamano, S.X. Nakamura, T.S.H. Lee, and T. Sato, Phys. Rev. C **88**, 035209 (2013).
[92] H. Kamano, S.X. Nakamura, T.S.H. Lee, and T. Sato, Phys. Rev. C **94**, 015201 (2016).
[93] S.X. Nakamura, H. Kamano, and T. Sato, Phys. Rev. D **92**, 074024 (2015).
[94] M. Ripani *et al.*, Phys. Rev. Lett. **91**, 022002 (2003).
[95] G.V. Fedotov *et al.*, Phys. Rev. C **79**, 015204 (2009).
[96] V.I. Mokeev *et al.*, Phys. Rev. C **80**, 045212 (2009).
[97] A. Anisovich, E. Klempt, A. Sarantsev, and U. Thoma, Eur. Phys. J. A **24**, 111 (2005).
[98] A.V. Anisovich, E. Klempt, V.A. Nikonov, A.V. Sarantsev, and U. Thoma, Eur. Phys. J. A **47**, 27 (2011).
[99] A.V. Anisovich *et al.*, Eur. Phys. J. A **48**, 15 (2012).
[100] A.V. Anisovich *et al.*, Eur. Phys. J. A **49**, 67 (2013).
[101] D. Rönchen *et al.*, Eur. Phys. J. A **51**, 70 (2015).
[102] SAID, http://gwdac.phys.gwu.edu and via ssh `ssh -X said@said.phys.gwu.edu` (2017).
[103] L. Tiator *et al.*, Phys. Rev. C **94**, 065204 (2016).
[104] M. Döring, J. Revier, D. Rönchen, and R.L. Workman, Phys. Rev. C **93**, 065205 (2016).
[105] J. Landay, M. Döring, C. Fernandez-Ramirez, B. Hu, and R. Molina, Phys. Rev. C **95**, 015203 (2017).